

Caspase-8 mediates caspase-1 processing and innate immune defense in response to bacterial blockade of NF- κ B and MAPK signaling

Naomi H. Philip^{a,b,1}, Christopher P. Dillon^c, Annelise G. Snyder^a, Patrick Fitzgerald^c, Meghan A. Wynosky-Dolfi^a, Erin E. Zwack^a, Baofeng Hu^a, Louise Fitzgerald^a, Elizabeth A. Mauldin^a, Alan M. Copenhaver^d, Sunny Shin^d, Lei Wei^e, Matthew Parker^f, Jinghui Zhang^f, Andrew Oberst^g, Douglas R. Green^c, and Igor E. Brodsky^{a,b,1}

^aDepartment of Pathobiology, University of Pennsylvania School of Veterinary Medicine, Philadelphia, PA 19104; ^bInstitute for Immunology and ^dDepartment of Microbiology, University of Pennsylvania Perelman School of Medicine, Philadelphia, PA 19104; Departments of ^cImmunology and ^fComputational Biology, St. Jude Children's Research Hospital, Memphis, TN 38105; ^eDepartment of Biostatistics and Bioinformatics, Roswell Park Cancer Institute, Buffalo, NY 14263; and ^gDepartment of Immunology, University of Washington, Seattle, WA 98109

Edited by Ruslan Medzhitov, Yale University School of Medicine, New Haven, CT, and approved April 1, 2014 (received for review February 25, 2014)

Toll-like receptor signaling and subsequent activation of NF- κ B and MAPK-dependent genes during infection play an important role in antimicrobial host defense. The YopJ protein of pathogenic *Yersinia* species inhibits NF- κ B and MAPK signaling, resulting in blockade of NF- κ B-dependent cytokine production and target cell death. Nevertheless, *Yersinia* infection induces inflammatory responses in vivo. Moreover, increasing the extent of YopJ-dependent cytotoxicity induced by *Yersinia pestis* and *Yersinia pseudotuberculosis* paradoxically leads to decreased virulence in vivo, suggesting that cell death promotes anti-*Yersinia* host defense. However, the specific pathways responsible for YopJ-induced cell death and how this cell death mediates immune defense against *Yersinia* remain poorly defined. YopJ activity induces processing of multiple caspases, including caspase-1, independently of inflammasome components or the adaptor protein ASC. Unexpectedly, caspase-1 activation in response to the activity of YopJ required caspase-8, receptor-interacting serine/threonine kinase 1 (RIPK1), and Fas-associated death domain (FADD), but not RIPK3. Furthermore, whereas RIPK3 deficiency did not affect YopJ-induced cell death or caspase-1 activation, deficiency of both RIPK3 and caspase-8 or FADD completely abrogated *Yersinia*-induced cell death and caspase-1 activation. Mice lacking RIPK3 and caspase-8 in their hematopoietic compartment showed extreme susceptibility to *Yersinia* and were deficient in monocyte and neutrophil-derived production of proinflammatory cytokines. Our data demonstrate for the first time to our knowledge that RIPK1, FADD, and caspase-8 are required for YopJ-induced cell death and caspase-1 activation and suggest that caspase-8-mediated cell death overrides blockade of immune signaling by YopJ to promote anti-*Yersinia* immune defense.

innate immunity | apoptosis | programmed necrosis | macrophage | pyroptosis

The innate immune response forms the first line of defense against pathogens. Microbial infection triggers the activation of pattern recognition receptors, such as Toll-like receptors (TLRs) on the cell surface or cytosolic nucleotide binding domain leucine-rich repeat family proteins (NLRs) (1). TLRs induce NF- κ B and MAPK signaling to direct immune gene expression, whereas certain NLRs direct the assembly of multiprotein complexes known as inflammasomes that provide platforms for caspase-1 or -11 activation (2). Active caspase-1 and -11 mediate cleavage and secretion of the IL-1 family of proteins and a proinflammatory cell death termed pyroptosis. However, microbial pathogens can interfere with various aspects of innate immune signaling, and the mechanisms that mediate effective immune responses against such pathogens remain poorly understood. Pathogenic *Yersiniae* cause diseases from gastroenteritis to plague and inject a virulence factor known as

YopJ, which inhibits NF- κ B and MAPK signaling pathways in target cells (2–4). YopJ activity inhibits proinflammatory cytokine production (4) and induces target cell death (5). YopJ activity induces processing of multiple caspases, including caspases-8, -3, -7, and -1 (6–8). Nevertheless, *Yersinia*-infected cells exhibit properties of both apoptosis and necrosis (9, 10), and no specific cellular factors have been identified as being absolutely required for YopJ-induced caspase activation and cell death. We previously found that the inflammasome proteins NLR CARD 4 (NLRC4), NLR Pyrin 3 (NLRP3), and apoptosis-associated speck-like protein containing a CARD (ASC), are dispensable for YopJ-induced caspase-1 processing and cell death (11). Thus, additional pathways likely mediate YopJ-induced caspase-1 activation and cell death.

Death receptors, such as TNF receptor and Fas, mediate caspase-8-dependent apoptosis via a death-inducing signaling complex containing receptor-interacting serine/threonine kinase 1 (RIPK1), caspase-8, and Fas-associated death domain (FADD) (12, 13). Whether these proteins are required for *Yersinia*-induced cell death, and whether this death contributes to antibacterial immune responses, is not known. The Ripoptosome complex, which contains RIPK1, FADD, caspase-8, as well as RIPK3 and cFLIP, regulates apoptosis, programmed necrosis,

Significance

Pathogenic organisms express virulence factors that can inhibit immune signaling pathways. Thus, the immune system is faced with the challenge of eliciting an effective inflammatory response to pathogens that actively suppress inflammation. The mechanisms that regulate this response are largely undefined. The *Yersinia* virulence factor YopJ blocks NF- κ B and MAPK signaling, resulting in reduced cytokine production and target cell death. Here, we find that caspase-8, RIPK1, and FADD are required for YopJ-induced cell death and show that mice lacking caspase-8 are severely susceptible to *Yersinia* infection and have defective proinflammatory cytokine production. These findings highlight a possible mechanism of immune defense that can overcome pathogen inhibition of cell-intrinsic proinflammatory immune responses.

Author contributions: N.H.P., C.P.D., D.R.G., and I.E.B. designed research; N.H.P., C.P.D., A.G.S., P.F., M.A.W.-D., E.E.Z., B.H., A.M.C., and I.E.B. performed research; L.W., M.P., J.Z., and A.O. contributed new reagents/analytic tools; N.H.P., C.P.D., L.F., E.A.M., S.S., D.R.G., and I.E.B. analyzed data; and N.H.P. and I.E.B. wrote the paper.

The authors declare no conflict of interest.

This article is a PNAS Direct Submission.

¹To whom correspondence may be addressed. E-mail: ibrodsky@vet.upenn.edu or nphilip@mail.med.upenn.edu.

This article contains supporting information online at www.pnas.org/lookup/suppl/doi:10.1073/pnas.1403252111/-DCSupplemental.

and survival in response to various stimuli including signaling by the TLR adaptor TRIF (14, 15). Because YopJ-induced cell death is inhibited in the absence of either TLR4 or TRIF (17) we sought to determine whether YopJ-dependent cell death and caspase-1 activation is regulated by caspase-8 or RIPK3 and to define the role of YopJ-dependent cell death in host defense. Here, we describe a previously unappreciated requirement for RIPK1, FADD, and caspase-8, but not RIPK3, in YopJ-induced caspase-1 activation and cell death. Critically, loss of caspase-8 in the hematopoietic compartment resulted in a failure of innate immune cells to produce proinflammatory cytokines in response to *Yersinia* infection and severely compromised resistance against *Yersinia* infection. Our data suggest that caspase-8-mediated cell death in response to blockade of NF- κ B/MAPKs by YopJ allows for activation of host defense against *Yersinia* infection. This cell death may thus enable the immune system to override inhibition of immune signaling by microbial pathogens.

Results

RIPK1 Is Required for *Yersinia*-Induced Cell Death and Caspase-1 Activation. Activation of multiple caspases, including caspase-1, -3, -7, and -8, is triggered owing to YopJ activity in *Yersinia*-infected cells (6, 7, 11, 16). *Casp1*^{-/-}*Casp11*^{-/-} bone marrow-derived macrophages (BMDMs) exhibit a significant delay in cell death in response to *Yersinia pseudotuberculosis* (Yp), whereas both Yp-induced cell death and caspase-1 activation are indistinguishable between B6 and *Casp11*^{-/-} or 129SvImJ BMDMs (Fig. S1 A–C and Table S1). These data suggest that caspase-1 plays a functional role in YopJ-induced cell death. Surprisingly, NLRC4, NLRP3, ASC, and type I IFN receptor alpha are dispensable for *Yersinia*-induced caspase-1 processing and cell death, suggesting that these events occur via a distinct pathway (Fig. S1 D–H and ref. 11).

RIPK1, RIPK3, caspase-8, and FADD regulate cell survival and death fate decisions downstream of TRIF as a result of RIP homotypic interaction motif-driven interactions between TRIF and RIPK1 (15, 19). This interaction can promote apoptosis through a RIPK1/FADD/caspase-8 complex (20), or programmed necrosis via RIPK1 and RIPK3 (21). We therefore investigated the potential involvement of RIPK1 in *Yersinia*-induced cell death. Necrostatin-1 (Nec-1) inhibits RIPK1 kinase activity and prevents TLR-induced necrosis (21, 22) but was previously reported not to inhibit *Yersinia pestis*-induced cell death (10). Surprisingly, we observed that both RIPK1-deficient BMDMs, and B6 BMDMs treated with Nec-1, exhibited reduced levels of Yp-induced caspase-1 and -8 processing (Fig. 1 A–D) and cell death (Fig. 1 E and F and Fig. S2 A and B). *Trif*^{-/-} BMDMs are partially protected from *Yersinia*-induced death (17). TLR4 signaling induces programmed necrosis in cells treated with the pan-caspase inhibitor zVAD-fmk via a TRIF- and RIPK3-dependent pathway (21). Interestingly, zVAD-fmk still sensitized *Trif*^{-/-} BMDMs to cell death in response to WT Yp, but not YopJ-deficient Yp (Δ YopJ) infection, whereas B6 BMDMs were sensitized to both (Fig. 1 E and F and Fig. S2 C). In contrast, *Ripk1*^{-/-} cells were not sensitized to death in the presence of zVAD-fmk in response to either Δ YopJ or Yp (Fig. 1 E and Fig. S2 D). These data indicate that YopJ induces cell death through RIPK1 via both TRIF-dependent and -independent pathways. Notably, although Nec-1 treatment protects Yp-infected cells from death, expression of NF- κ B-dependent cytokines was not restored (Fig. S2 E–G). These data demonstrate that YopJ-mediated blockade of cytokine production is independent of YopJ-induced cell death and imply that this cell death may serve an alternative function. Nec-1 did inhibit YopJ-induced secretion of IL-18, consistent with its effect on caspase-1 activation (Fig. 1 G). Altogether, these data demonstrate a key role for RIPK1 in *Yersinia*-induced death and caspase-1 activation and suggest that this cell death functions as a host defense against pathogen blockade of inflammatory signaling pathways.

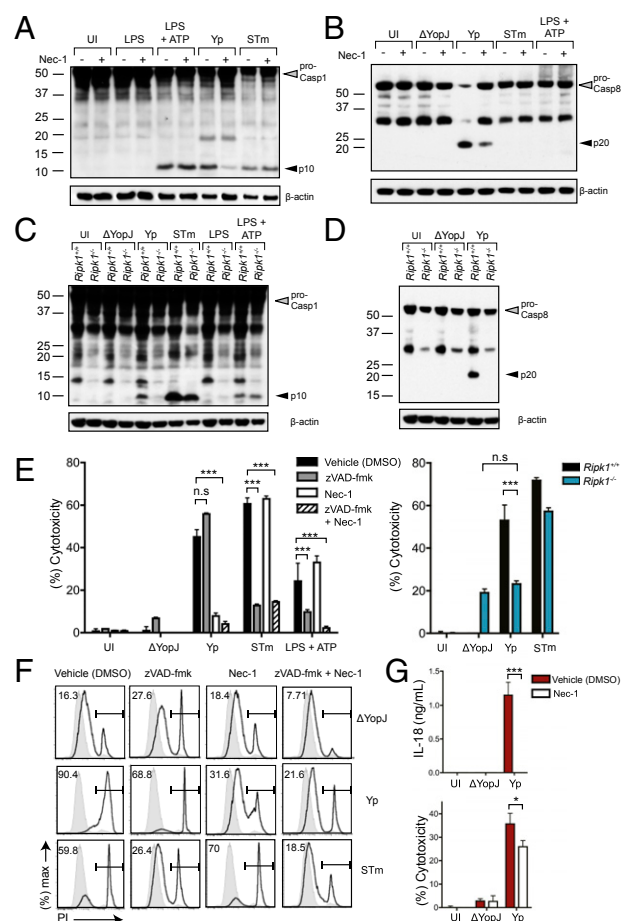


Fig. 1. RIPK1 is required for *Yersinia*-induced caspase-1 processing and cell death. (A and B) B6 BMDMs were either left uninfected (UI), LPS-primed (50 ng/mL) for 3 h followed by ATP (2.5 mM) for 1 h (LPS+ATP), or infected with WT *Yersinia* (Yp) or YopJ-deficient Yp (Δ YopJ) for 2 h or *Salmonella* (STm) for 1 h. Cell lysates were probed for caspase-1 or -8 processing by Western analysis. (C and D) *Ripk1*^{+/+} and *Ripk1*^{-/-} fetal liver-derived macrophages (FLDMs) were infected as in A and B. (E) Percent cytotoxicity was measured by LDH release from B6 BMDMs (Left) and *Ripk1*^{+/+} or *Ripk1*^{-/-} FLDMs (Right) that were uninfected or infected with Δ YopJ, Yp, or LPS+ATP for 4 h, or STm for 1 h. (F) Flow cytometry for PI uptake (percent PI⁺ cells) by cells as treated in E. (G) IL-18 assayed by ELISA and LDH release on cells treated as in E; 30 μ M Nec-1 and 100 μ M zVAD-fmk were used 3 h before infection where indicated. Grey peaks indicate uninfected cells. Error bars indicate mean \pm SEM of triplicates and are representative of three or more independent experiments. *** P < 0.0001, ** P < 0.001, * P < 0.01.

Caspase-8 Activity Is Required for YopJ-Induced Cell Death and Caspase-1 Processing. TLR signaling can trigger RIPK1-mediated cell death either via caspase-8 or RIPK3 (14, 21). The observation that zVAD-fmk-treatment did not protect B6 BMDMs from Yp-induced death suggests either caspases are not required for Yp-induced cell death or blocking caspase activity in Yp-infected cells triggers cell death via RIPK3-mediated necrosis. Caspase-8 catalytic activity prevents a lethal RIPK3-dependent programmed necrosis that occurs in early embryonic development (23). Notably, we found that *Ripk3*^{-/-} BMDMs had no defect in Yp-induced caspase-1 processing or cell death, whereas *Ripk3*^{-/-} *Casp8*^{-/-} BMDMs failed to process caspase-1 or undergo cell death in response to Yp infection, in contrast to *Salmonella* (STm) or LPS+ATP treatment (Fig. 2 A–C). This failure was not the result of insufficient back-crossing of these mice, because there were no single nucleotide variants between B6 and three different lines of 129 mice in caspase-8, cFLIP, FasL, or RIPK3, and the polymorphic genes immediately flanking caspase-8 are

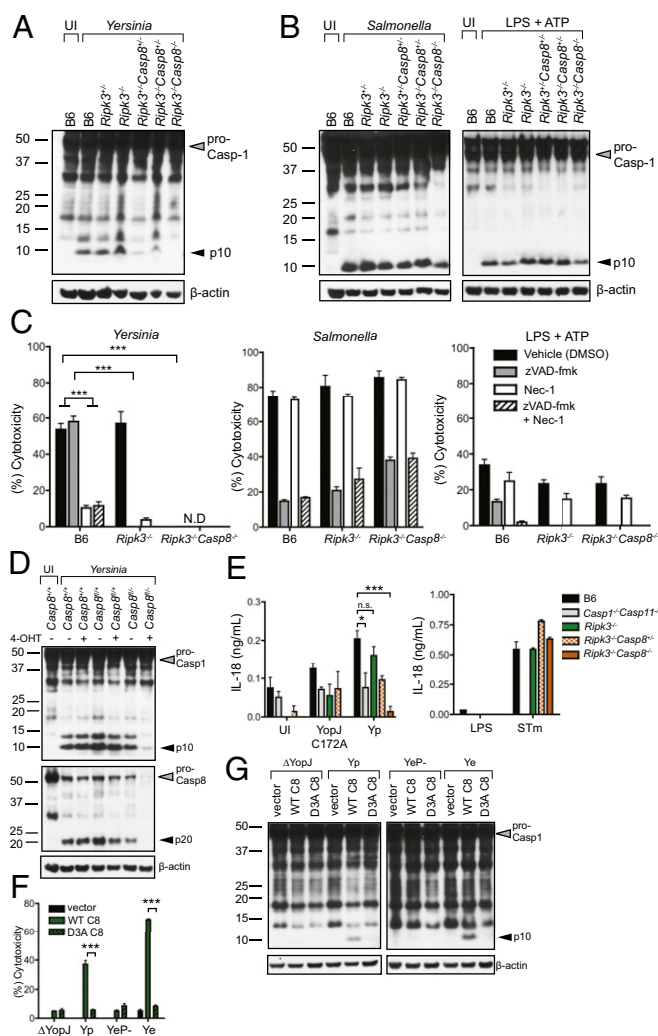


Fig. 2. Caspase-1 activation and IL-18 secretion in response to *Yersinia* infection require caspase-8. (A and B) Lysates from BMDMs left uninfected (UI), infected with Yp for 2 h, STm for 1 h, or LPS-primed for 3 h and ATP for 1 h (LPS+ATP) were probed for caspase-1 processing by Western analysis. (C) Percent cytotoxicity (LDH release) of BMDMs infected with Yp for 4 h, STm for 1 h, or treated with LPS+ATP as in A. (D) BMDMs treated with 4-hydroxytamoxifen (4-OHT) (50 nM) and infected as in A. (E) IL-18 assayed by ELISA from BMDMs left uninfected (UI), infected with isogenic Yp 32777, YopJ C172A, or STm, or LPS-primed for 4 h. (F and G) *iR3*^{-/-}*C8*^{-/-} BMDMs were reconstituted with empty vector, WT caspase-8 (WT C8), or noncleavable mutant caspase-8 (D3A C8). (F) LDH release 4 h postinfection. (G) Caspase-1 processing by Western analysis, MOI of 50:1; 30 μM Nec-1 and 100 μM zVAD-fmk were used 3 h before infection where indicated. N.D., not detected. Error bars indicate mean ± SEM of triplicates and are representative of three or more independent experiments. ***P < 0.0001.

not linked to these cell death pathways (Fig. S3). Importantly, in *Ripk3*^{-/-} BMDMs, zVAD-fmk abrogated Yp-induced death (Fig. 2C). These data demonstrate that caspase inhibition induces RIPK3-dependent programmed necrosis in Yp-infected cells and that RIPK3 is not required for YopJ-induced caspase-1 processing or cell death in the presence of caspase-8. RIPK3 can activate caspase-1 in the absence of caspase-8 in response to LPS (24) or cIAP inhibitors (25). Therefore, caspase-8 and RIPK3 might play redundant roles in caspase-1 activation or cell death during Yp infection. Intriguingly, conditional deletion of caspase-8 by inducible (ERT2-Cre), or developmental (LysM-Cre) approaches significantly reduced YopJ-mediated processing of

caspase-1 in RIPK3-sufficient cells, indicating that caspase-8 and RIPK3 play a nonredundant role in YopJ-induced caspase-1 processing (Fig. 2D and Fig. S4A). This caspase-8-dependent processing of caspase-1 was functionally important, because IL-18 secretion was significantly reduced in *Ripk3*^{-/-}*Casp8*^{-/-} but not in *Ripk3*^{-/-} BMDMs (Fig. 2E). However, conditional deletion of caspase-8 was not sufficient to protect BMDMs from Yp-induced cell death (Fig. S4B and C), in keeping with the finding that zVAD-fmk leads to programmed necrosis in RIPK3-sufficient cells. Importantly, caspase-1 activation in response to STm was completely unaffected in caspase-8 conditional BMDMs, indicating that these cells retained the ability to undergo inflammasome activation (Fig. S4D). We also observed an apparent synergy between zVAD-fmk and Nec-1 in protection from LPS+ATP-treated cell death in B6 cells (Fig. 2C). However, this is most likely because zVAD-fmk-pretreated cells that are then exposed to LPS+ATP undergo programmed necrosis, as *Ripk3*^{-/-} cells treated with zVAD-fmk followed by LPS+ATP are protected from cell death (Fig. 2C).

To dissect how caspase-8 mediates activation of caspase-1, we reconstituted immortalized *Ripk3*^{-/-}*Casp8*^{-/-} (*iR3*^{-/-}*C8*^{-/-}) macrophages with either WT caspase-8 (WT C8) or mutant caspase-8 lacking the three critical aspartate residues required for autoprocessing (D3A C8). Critically, expression of WT C8 but not of D3A C8 restored both Yp-induced cell death and processing of caspase-1 in *iR3*^{-/-}*C8*^{-/-} cells (Fig. 2F and G). Both forms of caspase-8 were expressed at similar levels in the reconstituted cells, but the D3A mutant lacked catalytic activity, consistent with observations that noncleavable forms of caspase-8 do not exhibit catalytic activity in the absence of forced dimerization (26) (Fig. S5A and B). Noncleavable caspase-8 nonetheless retains some function, because it interacts with cFLIP to inhibit programmed necrosis and mediate protection from embryonic lethality (23, 27). Consistently, zVAD-fmk treatment abolished both caspase-8 and caspase-1 processing in response to *Yersinia* infection, but not in STm-infected cells (Fig. S5C–E). These data indicate that zVAD-fmk does not block the autoprocessing of caspase-1 that occurs in canonical inflammasomes but inhibits caspase-8-mediated caspase-1 processing.

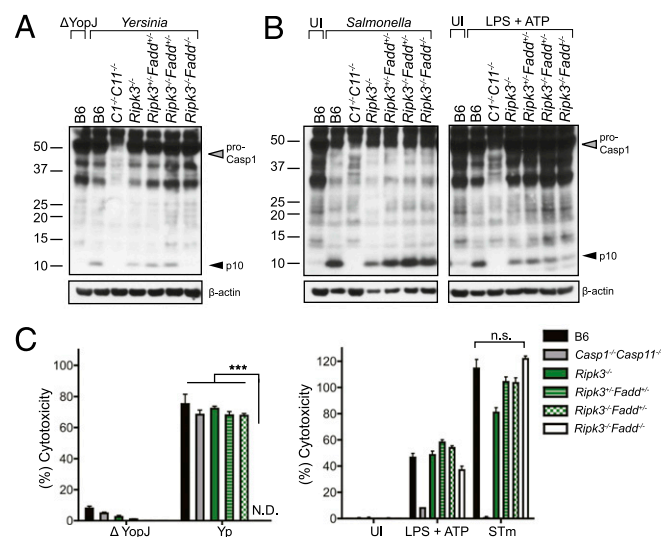


Fig. 3. FADD is required for *Yersinia*-induced caspase-1 processing and cell death in the absence of RIPK3. (A and B) BMDM cell lysates were probed for caspase-1 by Western analysis after infection with ΔYopJ or Yp for 2 h, STm for 1 h, treated with LPS for 3 h and ATP for 1 h (LPS+ATP), or left uninfected (UI). (C) Percent cytotoxicity (LDH release) of BMDMs left uninfected (UI), infected with ΔYopJ or Yp for 4 h, STm for 1 h, or LPS+ATP as in A. N.D., not detected. Error bars indicate mean ± SEM of triplicates and are representative of three or more independent experiments. ***P < 0.0001.

Altogether, these data indicate that the cleaved active caspase-8 homodimer mediates YopJ-induced processing of caspase-1.

Inhibition of NF- κ B and MAPK signaling by YopJ is necessary for Yp-induced cell death (28), but whether this is responsible for RIPK1- and caspase-8-mediated caspase-1 activation is not known. Intriguingly, inhibition of both $\text{I}\kappa\text{B}$ kinase beta (IKK β) and p38 MAPK induced RIPK1-dependent processing of caspase-8 and -1 and RIPK1-dependent death of Δ YopJ-infected cells (Fig. S6). Similarly to WT Yp infection, this cell death was largely unaffected in *Ripk3*^{-/-} cells but was abrogated in the absence of both RIPK3 and caspase-8. Together, these data demonstrate that YopJ-dependent inhibition of NF- κ B and MAPK signaling triggers RIPK1/caspase-8-mediated caspase-1 activation.

FADD Is Required for Yp-Induced Caspase-1 Processing and Cell Death. These findings, together with previous observations that YopP induces formation of a caspase-8, RIPK1, FADD complex (16), and that FADD plays a role in apoptosis downstream of TRIF (14), suggested that FADD might play a role in YopJ-induced caspase-1 activation and cell death. *Fadd*^{-/-} mice exhibit embryonic lethality that is reverted with loss of RIPK3 (29). As anticipated, YopJ-induced caspase-1 processing was indeed abrogated in *Ripk3*^{-/-}*Fadd*^{-/-} cells but not in *Ripk3*^{-/-} cells (Fig. 3A), whereas STm-infected cells exhibited robust caspase-1 processing in the absence of RIPK3 and FADD (Fig. 3A and B). Consistent with the recent study by Gurung et al. (30), *Ripk3*^{-/-}*Fadd*^{-/-} BMDMs also showed a noticeable reduction in LPS+ATP-induced caspase-1 processing and cell death (Fig. 3B and C). Moreover, proinflammatory cytokine production in response to LPS alone was reduced in BMDMs lacking RIPK3 and caspase-8 or FADD (Fig. S7), consistent with recent findings that pro-IL-1 β expression is reduced in these cells (30–32). Whereas Gurung et al. (30) observed that caspase-8 contributes to LPS+ATP-induced canonical inflammasome activation, unlike with FADD deficiency, we did not observe a consistent reduction in caspase-1 processing in *Ripk3*^{-/-}*Casp8*^{-/-} macrophages treated with LPS+ATP, and we were unable to detect caspase-8

processing in LPS+ATP-treated cells. The contribution of FADD and caspase-8 to LPS+ATP-induced caspase-1 activation may relate to differential effects on NLRP3 inflammasome priming.

YopJ-Induced Caspase-8 Activation Promotes Anti-Yersinia Immune Defense in Vivo. YopJ promotes dissemination of *Yersinia* to systemic tissues (33). However, increasing YopJ-mediated cytotoxicity paradoxically enhances immune clearance and reduces virulence (34). How this cytotoxicity contributes to host defense in vivo is not known. We therefore infected bone marrow chimeric mice lacking both RIPK3 and caspase-8 in the hematopoietic compartment, because these cells cannot undergo YopJ-induced cell death. Critically, in contrast to B6, *Ripk3*^{-/-}, or littermate control bone marrow (BM) chimeras, mice with a caspase-8-deficient hematopoietic compartment rapidly succumbed to infection with a Yp strain that is nonlethal to WT mice (35) (Fig. 4A and Fig. S8A). Surprisingly, *Ripk3*^{-/-}*Casp8*^{-/-} chimeric mice were deficient in production of serum IFN- γ , IL-6, and IL-1 β despite a several-log increase in bacterial cfu in infected tissues on day 6 postinfection, (Fig. 4B and C and Fig. S8B). Both innate and adaptive *Ripk3*^{-/-}*Casp8*^{-/-} cells failed to produce cytokines; inflammatory monocytes in the mesenteric lymph nodes (mLNs) and splenic natural killer (NK) cells were all defective in production of TNF- α , and IFN- γ at day 6 postinfection (Fig. 4D–G and Fig. S8C). In contrast, the chemokine MCP-1 was not affected in *Ripk3*^{-/-}*Casp8*^{-/-} chimeric mice (Fig. 4B). On day 3 postinfection, *Ripk3*^{-/-}*Casp8*^{-/-} chimeras had a higher proportion of TNF-producing inflammatory monocytes in the spleen (Fig. S9B), suggesting that caspase-8 deficiency in vivo does not lead to a failure of cell-intrinsic cytokine production per se. Cytokine production in the mLNs, where bacterial burdens were similar across genotypes, was defective on both days 3 and 5 (Fig. S9A–C).

These findings demonstrate that combined deficiency of RIPK3 and caspase-8 results in severe susceptibility to WT Yp infection, but whether this is due to a failure to respond to the activity of YopJ or to a more global failure to induce immune responses was not clear. Importantly, *Ripk3*^{-/-}*Casp8*^{-/-} bone marrow chimeric animals were capable of surviving infection

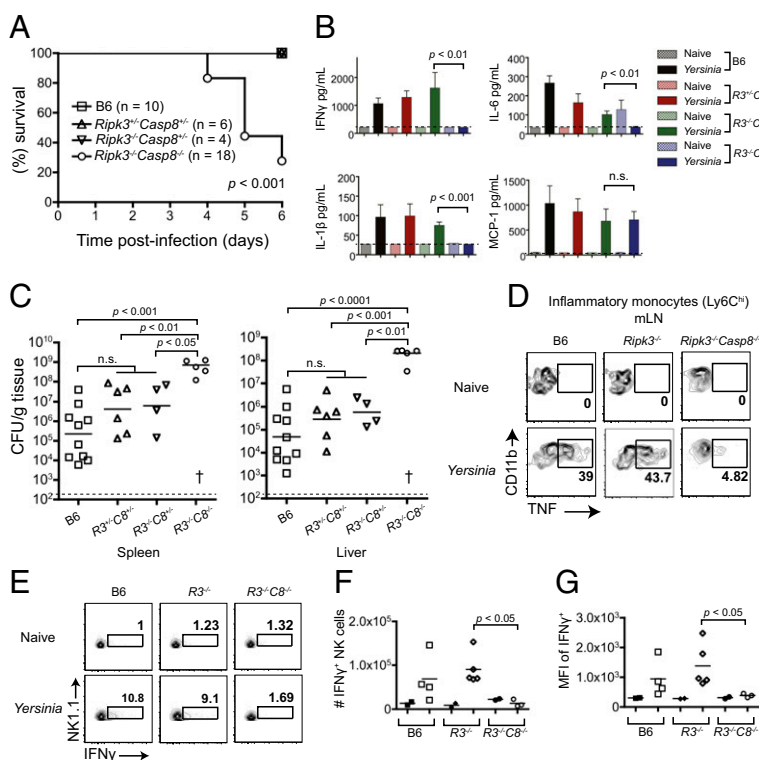


Fig. 4. RIPK3/caspase-8-deficient mice are highly susceptible to *Yersinia* infection and have dysregulated cytokine production. Lethally irradiated B6.SJL mice were reconstituted with B6, *Ripk3*^{+/+}*Casp8*^{+/+}, *Ripk3*^{-/-}*Casp8*^{+/+}, *Ripk3*^{-/-}, or *Ripk3*^{-/-}*Casp8*^{-/-} BM and orally infected with $8\text{--}10 \times 10^7$ cfu *Yersinia* (Yp) per mouse. Mice were assayed for (A) survival, (B) serum IFN- γ , IL-6, IL-1 β , and MCP-1 by Luminex, (C) bacterial loads per gram of tissue, and (D) percent TNF⁺ inflammatory monocytes in mLNs by flow cytometry. (E–H) IFN- γ production from splenic NK cells (NK1.1⁺) was assessed by flow cytometry. (E) Representative plots, (F) total numbers, and (G) mean fluorescence intensity (MFI). (B–G) Day 6 postinfection. Dagger denotes 13 dead or moribund mice not harvested for cfus. Dotted lines represent limit of detection. Solid lines represent means (ELISA) or geometric means (cfu). Flow cytometry plots in D were gated on live CD45.2⁺, CD11c⁺, CD11b^{hi}, Ly6G⁺, and Ly6C^{hi} cells and in E–G on live CD45.2⁺ CD3⁺ cells. *R3C8*, *Ripk3Casp8*. Statistical analysis in F and G was performed using the Mann–Whitney *U* test. Data representative of two or more independent experiments.

with Δ YopJ Yp, had significantly lower bacterial burdens of Δ YopJ in their spleen and liver, and partially recovered production of intracellular TNF (Fig. 5 A–C). Despite elevated bacterial burdens, in the $Ripk3^{-/-}Casp8^{-/-}$ chimeras these mice had smaller splenic lesions that lacked close association of neutrophils with bacteria, compared with control caspase-8-sufficient chimeras, which had extensive lesions containing bacterial colonies surrounded by visible cell debris and neutrophilic infiltrates (Fig. 5D, Fig. S9 D and E, and Table S2). These data are consistent with reduced levels of in vivo death of $Ripk3^{-/-}Casp8^{-/-}$ cells. Intriguingly, Δ YopJ-infected $Ripk3^{-/-}Casp8^{-/-}$ chimeras showed significantly elevated numbers and extent of liver lesions compared with Yp-infected animals, suggesting that in the absence of NF- κ B blockade the $Ripk3^{-/-}Casp8^{-/-}$ cells can generate protective inflammatory responses that correlate with increased cell death in vivo (Fig. 5 E–G). Together these findings demonstrate that YopJ-dependent triggering of caspase-8 plays a critical role in mediating anti-*Yersinia* immune defense in vivo and that loss of RIPK3 and caspase-8 results in dysregulated inflammatory responses and failure to control *Yersinia*.

Discussion

Caspase-1 and caspase-8 activation are generally induced by distinct stimuli. In contrast to caspase-1, which causes pyroptosis independently of other caspases, caspase-8 induces apoptosis through caspases-3 and -7. Caspase-8 can also mediate cleavage and secretion of IL-1 β and IL-18 downstream of Fas/FasL

signaling or endoplasmic reticulum stress (36, 37) and was recently reported to regulate expression of pro-IL-1 β (31, 32). We now demonstrate that caspase-8, RIPK1, and FADD mediate caspase-1 activation in response to the *Yersinia* virulence factor YopJ, thus revealing an unanticipated integration of caspase-1 and caspase-8 death pathways in response to *Yersinia* infection.

We cannot currently exclude the possibility that RIPK3 and caspase-8 function redundantly to mediate cell death, or that RIPK3-mediated necrosis contributes to host defense against *Yersinia*. Nevertheless, in caspase-8-sufficient cells, RIPK3 is dispensable for YopJ-induced cell death or caspase-1 activation, and in caspase-8 conditional knockout cells, RIPK3 is not sufficient for YopJ-induced caspase-1 processing. Under certain conditions, RIPK3 can mediate caspase-1 activation and cell death in response to LPS (24) or cIAP inhibitors (25). Thus, whereas TLR stimulation alone triggers RIPK3-dependent necrosis in caspase-8-deficient cells, our data demonstrate that YopJ triggers cell death and caspase-1 processing through caspase-8. Engagement of caspase-1 by both of these pathways may enable the release of caspase-1-dependent inflammatory signals by dying cells, even when this caspase-1 activation does not occur in a canonical inflammasome platform. Our data suggest a model (Fig. S10) whereby RIPK1, caspase-8, and FADD engage a cell death and caspase-1-activation pathway that promotes antimicrobial immune defense in response to pathogen-mediated interference with innate immune signaling pathways.

In addition to controlling cell-extrinsic death, caspase-8 also plays a role in NF- κ B signaling and gene expression (31, 32, 38, 39), potentially via cleavage of cFLIP (40, 41). However, YopJ-induced caspase-1 activation and cell death via caspase-8 and FADD are independent of LPS-induced priming, because they are triggered by NF- κ B inhibition and are independent of ASC, NLRP3, and IFNAR. Indeed, LPS priming prevents YopJ-driven cell death (6, 11), either owing to up-regulation of NF- κ B-dependent survival genes or inhibition of caspase-1 by YopM in LPS-primed cells (42).

A previous study by Zheng et al. (43) observed a role for ASC in caspase-1 activation in *Y. pestis*-infected cells, in contrast to our studies here. YopJ isoforms from different *Yersinia* isolates exhibit different degrees of NF- κ B inhibitory activity, and this also correlates with their degree of ASC/NLRP3 inflammasome activation. An alternative possibility is the slightly different infection conditions in the Zheng et al. study, which infected cells for 20 min prior to gentamicin treatment. Future studies will dissect the underlying basis for this apparent difference.

Finally, whether cell death or dysregulated cytokine production, or both, are directly responsible for the inability of caspase-8-deficient animals to clear *Yersinia* infection remains to be determined. The drop in cytokine production over the course of Yp infection in $Ripk3^{-/-}Casp8^{-/-}$ chimeric mice may be due to increased blockade of signaling pathways as a consequence of progressively greater bacterial burden over time. Caspase-8-mediated cell death and caspase-1 activation in response to blockade of innate signaling may thus mobilize bystander cells for rapid cytokine production and/or phagocytosis of pathogen-associated cell debris.

Materials and Methods

Cell Culture and Infections. BMDMs were grown and infected as previously described (11). Briefly, *Yersinia* were grown overnight with aeration in 2xYT broth at 26 °C. On the next day, *Yersinia* were diluted into inducing media and grown with aeration for 1 h at 26 °C followed by 2 h at 37 °C. *Salmonella* was grown overnight in LB at 37 °C with aeration, then diluted into high-salt LB and grown standing at 37 °C. Cells were infected at a multiplicity of infection (MOI) of 20:1, centrifuged at 200 \times g for 5 min, gentamicin (100 μ g/mL) was added 1 h after infection, and cells/supernatants were harvested at indicated time points. Caspase processing in cell lysates was analyzed by Western blotting, percent cytotoxicity was assayed by lactate dehydrogenase (LDH) release or propidium iodide (PI) uptake, and release of cytokines was analyzed by ELISA as described in SI Text. All statistical analyses were performed using the two-tailed unpaired Student *t* test.

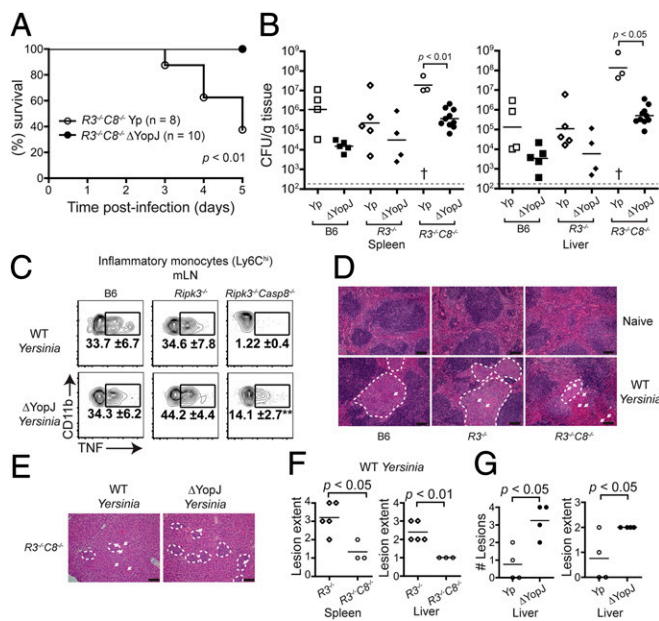


Fig. 5. RIPK3/caspase-8-deficient mice survive Δ YopJ infection and partially recover intracellular cytokine production. Lethally irradiated B6.SJL mice were reconstituted with B6, $Ripk3^{-/-}$, or $Ripk3^{-/-}Casp8^{-/-}$ BM and orally infected with $8-10 \times 10^7$ cfu *Yersinia* (Yp) or Δ YopJ *Yersinia* (Δ YopJ) per mouse. Mice were assayed for (A) survival, (B) bacterial loads per gram of tissue, and (C) percent TNF⁺ inflammatory monocytes in mLNs by flow cytometry. (D and E) Representative images of H&E-stained (D) spleen and (E) liver sections in naïve and infected chimeric mice, showing lesions of necrosuppurative inflammation (dashed white lines) and extracellular bacterial colonies (arrows) in infected mice. (Scale bars, 50 μ m.) (F and G) Quantification of number and extent of lesions. (B) Day 5. (C) Representative plots from pooled data on days 5 and 6 (% \pm SEM). (D–G) Day 6. Dagger denotes five dead or moribund mice not harvested for cfus. Dotted lines represent limit of detection. Solid lines represent means (histology) or geometric means (cfu). Flow cytometry plots were gated on live CD45.2⁺, CD11c⁺, CD11b^{hi}, Ly6G⁺, Ly6C^{hi} cells. ***P* < 0.01, WT vs. Δ YopJ infected $Ripk3^{-/-}Casp8^{-/-}$ monocytes. R3C8, $Ripk3Casp8$. Data representative of two or more independent experiments.

Animal Infections. Mice (fasted 12–16 h) were orally inoculated with $8\text{--}10 \times 10^7$ *Yersinia* (32777). Tissues and sera were collected on days 3, 5, and 6. Tissues were processed and plated on LB plates containing irgasan ($2 \mu\text{g/mL}$) to determine bacterial loads (colony-forming units per gram). Levels of serum cytokines were assayed by Luminex. Cells from spleens and mesenteric lymph nodes were cultured in the presence of brefeldin A and monensin for 5 h, stained for surface and intracellular cytokines, and analyzed by flow cytometry as described in *SI Text*. Spleen sections were fixed and stained for H&E. All animal studies were performed in accordance with University of Pennsylvania Institutional Animal Care and Use Committee approved protocols.

ACKNOWLEDGMENTS. We thank Gordon Ruthel of the PennVet Imaging Core, the Flow Cytometry and Cell Sorting Core, and Human Immunology Core for technical assistance. We thank Vishva Dixit (Genentech) for *Ripk3*^{−/−} mice and Razq Hakem (University Health Network) for *Casp8*^{fl/fl} mice. Junying Yuan and Tiffany Horng (Harvard University) provided *Casp11*^{−/−} BM; Thirumala Devi-Kanneganti (St. Jude Children's Research Hospital) provided *Casp3*^{−/−} and *Casp7*^{−/−} BM; *Casp8*^{fl/fl} × *LysM-Cre* BM was provided by Stephen Hedrick (University of California at San Diego); and Jim Bliska (State University of New York, Stony Brook) provided *Yersinia* strains. We thank Lance Peterson for critical reading. This work was supported in part by a Pilot Award from the University Research Foundation and National Institutes of Health Grants AI109267 and AI103062 (to I.E.B.).

- Medzhitov R (2007) Recognition of microorganisms and activation of the immune response. *Nature* 449(7164):819–826.
- Broz P, Monack DM (2013) Newly described pattern recognition receptors team up against intracellular pathogens. *Nat Rev Immunol* 13(8):551–565.
- Mukherjee S, et al. (2006) *Yersinia* YopJ acetylates and inhibits kinase activation by blocking phosphorylation. *Science* 312(5777):1211–1214.
- Orth K, et al. (1999) Inhibition of the mitogen-activated protein kinase superfamily by a *Yersinia* effector. *Science* 285(5435):1920–1923.
- Palmer LE, Hobbie S, Galán JE, Bliska JB (1998) YopJ of *Yersinia pseudotuberculosis* is required for the inhibition of macrophage TNF- α production and downregulation of the MAP kinases p38 and JNK. *Mol Microbiol* 27(5):953–965.
- Monack DM, Mecsas J, Ghori N, Falkow S (1997) *Yersinia* signals macrophages to undergo apoptosis and YopJ is necessary for this cell death. *Proc Natl Acad Sci USA* 94(19):10385–10390.
- Bergsbaken T, Cookson BT (2007) Macrophage activation redirects *Yersinia*-infected host cell death from apoptosis to caspase-1-dependent pyroptosis. *PLoS Pathog* 3(11):e161.
- Denecker G, et al. (2001) *Yersinia enterocolitica* YopP-induced apoptosis of macrophages involves the apoptotic signaling cascade upstream of bid. *J Biol Chem* 276(23):19706–19714.
- Lilo S, Zheng Y, Bliska JB (2008) Caspase-1 activation in macrophages infected with *Yersinia pestis* KIM requires the type III secretion system effector YopJ. *Infect Immun* 76(9):3911–3923.
- Gröbner S, et al. (2006) *Yersinia* YopP-induced apoptotic cell death in murine dendritic cells is partially independent from action of caspases and exhibits necrosis-like features. *Apoptosis* 11(11):1959–1968.
- Zheng Y, Lilo S, Mena P, Bliska JB (2012) YopJ-induced caspase-1 activation in *Yersinia*-infected macrophages: Independent of apoptosis, linked to necrosis, dispensable for innate host defense. *PLoS ONE* 7(4):e36019.
- Brodsky IE, et al. (2010) A *Yersinia* effector protein promotes virulence by preventing inflammasome recognition of the type III secretion system. *Cell Host Microbe* 7(5):376–387.
- Muzio M, et al. (1996) FLICE, a novel FADD-homologous ICE/CED-3-like protease, is recruited to the CD95 (Fas/APO-1) death-inducing signaling complex. *Cell* 85(6):817–827.
- Vandenabeele P, Declercq W, Van Herreweghe F, Vanden Berghe T (2010) The role of the kinases RIP1 and RIP3 in TNF-induced necrosis. *Sci Signal* 3(115):re4.
- Feoktistova M, et al. (2011) cIAPs block Ripoptosome formation, a RIP1/caspase-8 containing intracellular cell death complex differentially regulated by cFLIP isoforms. *Mol Cell* 43(3):449–463.
- Feoktistova M, Geserick P, Panayotova-Dimitrova D, Leverkus M (2012) Pick your poison: The Ripoptosome, a cell death platform regulating apoptosis and necroptosis. *Cell Cycle* 11(3):460–467.
- Zhang Y, Bliska JB (2003) Role of Toll-like receptor signaling in the apoptotic response of macrophages to *Yersinia* infection. *Infect Immun* 71(3):1513–1519.
- Gröbner S, et al. (2007) Catalytically active *Yersinia* outer protein P induces cleavage of RIP and caspase-8 at the level of the DISC independently of death receptors in dendritic cells. *Apoptosis* 12(10):1813–1825.
- Green DR, Oberst A, Dillon CP, Weinlich R, Salvesen GS (2011) RIPK-dependent necrosis and its regulation by caspases: a mystery in five acts. *Mol Cell* 44(1):9–16.
- Kaiser WJ, Offermann MK (2005) Apoptosis induced by the toll-like receptor adaptor TRIF is dependent on its receptor interacting protein homotypic interaction motif. *J Immunol* 174(8):4942–4952.
- He S, Liang Y, Shao F, Wang X (2011) Toll-like receptors activate programmed necrosis in macrophages through a receptor-interacting kinase-3-mediated pathway. *Proc Natl Acad Sci USA* 108(50):20054–20059.
- Degterev A, et al. (2008) Identification of RIP1 kinase as a specific cellular target of necrostatins. *Nat Chem Biol* 4(5):313–321.
- Oberst A, et al. (2011) Catalytic activity of the caspase-8-FLIP(L) complex inhibits RIPK3-dependent necrosis. *Nature* 471(7338):363–367.
- Kang TB, Yang SH, Toth B, Kovalenko A, Wallach D (2013) Caspase-8 blocks kinase RIPK3-mediated activation of the NLRP3 inflammasome. *Immunity* 38(1):27–40.
- Vince JE, et al. (2012) Inhibitor of apoptosis proteins limit RIP3 kinase-dependent interleukin-1 activation. *Immunity* 36(2):215–227.
- Pop C, Fitzgerald P, Green DR, Salvesen GS (2007) Role of proteolysis in caspase-8 activation and stabilization. *Biochemistry* 46(14):4398–4407.
- Kang TB, et al. (2004) Caspase-8 serves both apoptotic and nonapoptotic roles. *J Immunol* 173(5):2976–2984.
- Zhang Y, Ting AT, Marcu KB, Bliska JB (2005) Inhibition of MAPK and NF- κ B pathways is necessary for rapid apoptosis in macrophages infected with *Yersinia*. *J Immunol* 174(12):7939–7949.
- Dillon CP, et al. (2012) Survival function of the FADD-CASPASE-8-cFLIP(L) complex. *Cell Rep* 1(5):401–407.
- Gurung P, et al. (2014) FADD and caspase-8 mediate priming and activation of the canonical and noncanonical Nlrp3 inflammasomes. *J Immunol* 192(4):1835–1846.
- Antonopoulos C, El Sanadi C, Kaiser WJ, Mocarski ES, Dubyak GR (2013) Proapoptotic chemotherapeutic drugs induce noncanonical processing and release of IL-1 β via caspase-8 in dendritic cells. *J Immunol* 191(9):4789–4803.
- Man SM, et al. (2013) Salmonella infection induces recruitment of Caspase-8 to the inflammasome to modulate IL-1 β production. *J Immunol* 191(10):5239–5246.
- Monack DM, Mecsas J, Bouley D, Falkow S (1998) *Yersinia*-induced apoptosis in vivo aids in the establishment of a systemic infection of mice. *J Exp Med* 188(11):2127–2137.
- Brodsky IE, Medzhitov R (2008) Reduced secretion of YopJ by *Yersinia* limits in vivo cell death but enhances bacterial virulence. *PLoS Pathog* 4(5):e1000067.
- McPhee JB, Mena P, Zhang Y, Bliska JB (2012) Interleukin-10 induction is an important virulence function of the *Yersinia pseudotuberculosis* type III effector YopM. *Infect Immun* 80(7):2519–2527.
- Bossaller L, et al. (2012) Cutting edge: FAS (CD95) mediates noncanonical IL-1 β and IL-18 maturation via caspase-8 in an RIP3-independent manner. *J Immunol* 189(12):5508–5512.
- Shenderov K, et al. (2014) Cutting edge: Endoplasmic reticulum stress licenses macrophages to produce mature IL-1 β in response to TLR4 stimulation through a caspase-8 and TRIF-dependent pathway. *J Immunol* 192(5):2029–2033.
- Lemmers B, et al. (2007) Essential role for caspase-8 in Toll-like receptors and NF- κ B signaling. *J Biol Chem* 282(10):7416–7423.
- Su H, et al. (2005) Requirement for caspase-8 in NF- κ B activation by antigen receptor. *Science* 307(5714):1465–1468.
- Golks A, Brenner D, Krammer PH, Lavrik IN (2006) The c-FLIP-NH2 terminus (p22-FLIP) induces NF- κ B activation. *J Exp Med* 203(5):1295–1305.
- Koenig A, et al. (2014) The c-FLIP cleavage product p43FLIP promotes activation of extracellular signal-regulated kinase (ERK), nuclear factor κ B (NF- κ B), and caspase-8 and T cell survival. *J Biol Chem* 289(2):1183–1191.
- LaRock CN, Cookson BT (2012) The *Yersinia* virulence effector YopM binds caspase-1 to arrest inflammasome assembly and processing. *Cell Host Microbe* 12(6):799–805.
- Zheng Y, et al. (2011) A *Yersinia* effector with enhanced inhibitory activity on the NF- κ B pathway activates the NLRP3/ASC/caspase-1 inflammasome in macrophages. *PLoS Pathog* 7(4):e1002026.

Supporting Information

Philip et al. 10.1073/pnas.1403252111

SI Text

Cell Culture and Infection Conditions. Bone marrow-derived macrophages (BMDMs) were grown as previously described (1) in a 37 °C humidified incubator in DMEM supplemented with 10% FBS, Hepes, sodium pyruvate (complete DMEM), and 30% L929 supernatant for 7–9 d. Receptor interacting protein kinase 3-deficient (*Ripk3*^{−/−}) mice are N7 generation back-crossed and were provided by Vishva M. Dixit, Genentech, San Francisco. Caspase-8 (*Casp8*^{fl}) mice were provided by Razq Hakem, University Health Network, Toronto; Fas-associated death domain protein-deficient (*Fadd*^{−/−}) mice were provided by Tak W. Mak, University Health Network, Toronto; and *Ripk1*^{−/−} mice were provided by Michele Kelliher, University of Massachusetts, Boston. *Ripk3*^{−/−}*Casp8*^{−/−} mice in these studies were back-crossed six times and a detailed SNP analysis of *Ripk3*^{−/−}*Fadd*^{−/−} mice indicated that 90–94% of loci are B6 in any given mouse. Bones from *Casp3*^{−/−} and *Casp7*^{−/−} mice were provided by T. Devi-Kanneganti, St. Jude Children's Research Hospital, or purchased from Jackson Laboratories. Bones from *Trif*^{−/−} mice were provided by Sankar Ghosh, Columbia University, New York, and bones from *MyD88*^{−/−} mice were provided by Ruslan Medzhitov, Yale University, New Haven, CT. *Casp8*^{fl/fl}*xLysM-Cre* bones were provided by Stephen Hedrick, University of California at San Diego, La Jolla. Fetal liver-derived macrophages (FLDMs) were grown from E12–14 livers in complete DMEM and 50% L929 supernatant for 7–9 d. Sixteen to twenty hours before infection cells were replated into 96-, 48-, 24-, or 12-well dishes in complete DMEM containing 10% L929 supernatant. Bacterial strains are described in Table S1. *Yersinia* were grown overnight with aeration in 2×YT broth at 26 °C. The bacteria were diluted into fresh 2×YT containing 20 mM sodium oxalate and 20 mM MgCl₂ (inducing media). Bacteria were grown with aeration for 1 h at 26 °C followed by 2 h at 37 °C. *Salmonella* were grown overnight in LB medium at 37 °C with aeration, diluted into fresh LB containing 300 mM NaCl, and grown standing at 37 °C for 3 h. Bacteria were washed three times with prewarmed DMEM, added to the cells at a multiplicity of infection (MOI) of 20:1 unless otherwise indicated, and spun onto the cells at 1,000 rpm for 5 min. Cells were incubated at 37 °C for 1 h post-infection followed by addition of 100 µg/mL gentamicin. Necrostatin-1 (Nec-1) and zVAD-fmk were added 2 or 3 h before infection [30 µM or 60 µM Nec-1 (Calbiochem), 100 µM zVAD-fmk-001 (R & D Systems), 0.5 µg/mL Cytochalasin-D (Sigma), and 25 mM N-acetylcysteine (Sigma)]. IκB kinase beta (IKKβ) and p38 inhibitors were added 1 h before infection (BMS 345541 and SB202190; Millipore).

4-Hydroxytamoxifen Treatment. The 4-hydroxytamoxifen (4-OHT) (50 nM, 98% pure Z-form; Sigma) was added on days 3 and 5 to indicated BMDMs in complete DMEM supplemented with 30% L929 supernatant. Cells were replated on day 7 and infections were performed as described above on day 8.

Western Blotting. All *Yersinia* infections, unless otherwise indicated, were performed with wild type *Yersinia pseudotuberculosis* strain IP2666 (Yp) or YopJ-deficient *Yersinia pseudotuberculosis* IP26 (ΔYopJ). Cell lysates were analyzed by Western blotting as described in ref. 1. Briefly, cells were lysed in 20 mM Hepes, 150 mM NaCl, 10% glycerol, 1% Triton X-100, and 1 mM EDTA. Lysates were mixed with protein loading buffer, boiled, and centrifuged and 20% of the total cell lysate loaded onto 4–12% NuPAGE gels (Invitrogen). Proteins were transferred to PVDF membrane (Millipore) and blotted with rabbit anti-

mouse caspase-1 antibody (sc-514; Santa Cruz Biotechnology), rat anti-mouse caspase-8 (clone 1G12, ALX 804-447-C100; Enzo Life Sciences), or mouse anti-mouse β-actin (Sigma). Secondary antibodies were goat anti-rabbit, goat anti-rat (Jackson ImmunoResearch), or anti-mouse HRP (Cell Signaling Technology). Concentrations for lysis were calculated based on vol/vol.

Generation of Immortalized Cell Line. Freshly isolated *Ripk3*^{−/−}*Casp8*^{−/−} bone marrow was infected with the v-myc/v-raf expressing J2-Cre retrovirus (2) and differentiated in 15% L929 supernatant. After 20 d in culture macrophages were weaned off L929 and passaged in complete-DMEM.

Viral Transductions. WT C8 expression was accomplished by cloning full-length murine caspase-8 into the pBabe-Puro retroviral vector upstream of the T2A ribosomal skipping sequence followed by enhanced GFP. Mutations in murine D3A C8 were inserted at D387A, D397A, and D400A using the QuikChange Site Directed Mutagenesis kit (Agilent). D3A C8 was cloned into the pRRL-Puro lentiviral vector upstream of the T2A ribosomal skipping sequence followed by enhanced GFP. Stable expression was achieved by retro- or lentiviral transduction of *iR3*^{−/−}*C8*^{−/−} cells followed by two rounds of sorting by FACS to enrich for GFP⁺ cells. Plasmids were a gift from A.O.

Cell Death Assays. Lactate dehydrogenase release. All *Yersinia* infections, unless otherwise indicated (as in Fig. 1G and Figs. S1B and S6) were performed with IP2666 (Yp) or IP26 (ΔYopJ). BMDMs were seeded into 96-well plates at a density of 7 × 10⁴ cells per well in complete DMEM containing 10% L929 supernatant. Cells were infected as described above and supernatants harvested at indicated times postinfection. Lactate dehydrogenase (LDH) release was quantified using the Cytotox96 Assay Kit (Promega) according to the manufacturer's instructions. Cytotoxicity was normalized to Triton (100%) and LDH release from uninfected/untreated cells was used for background subtraction.

Propidium iodide uptake was analyzed by flow cytometry and confocal microscopy. Cells were seeded in 12-well suspension dishes at a density of 5 × 10⁵ cells per well 16–20 h prior to infection. Cells were harvested with cold PBS at indicated times, washed twice with PBS, and stained with propidium iodide (PI) (Calbiochem), washed twice with PBS, run on an LSR Fortessa, and analyzed using FlowJo (TreeStar) software.

Kinetics of PI uptake was analyzed by time-lapse confocal microscopy. Twelve-well chamber slides (ibidi) were coated with 1 mg/mL poly-L-lysine (Sigma) at 4 °C 1 d before seeding cells. Cells were seeded at a density of 8–10 × 10⁴ cells per well 16–20 h before infection. Four hours before infection, cells were loaded with Cell Tracker Green (Invitrogen) according to manufacturer's instructions, washed once, and replenished with fresh media. At time of infection, PI was added and PI uptake was analyzed using the inverted Leica DMI4000 based Yokagawa CSUX-1 spinning disk confocal microscope in a 37 °C humidified chamber (Penn Vet Imaging Core) over indicated time points.

ELISAs and Luminex. BMDMs were pretreated with 50 ng/mL *Escherichia coli* LPS (Sigma) for 3 h before bacterial infection as described above, and supernatants were harvested 4 h post-infection. Release of proinflammatory cytokines was measured by ELISA using capture and detection antibodies against IL-6, IL-12, IL-1α (BD Pharmingen), or IL-1β (e-Bioscience). To

detect IL-18 by ELISA (MBL International) from *Yersinia*-infected cells, BMDMs were infected (with LPS priming where indicated) and supernatants were harvested 4 h postinfection. Magnetic 20-plex Luminex (Invitrogen) was performed at the University of Pennsylvania Human Immunology Core to quantify cytokines and chemokines in mouse serum.

Caspase-8 Activity Assay. BMDMs were seeded into 96-well white-walled plates at a density of 7×10^4 cells per well in complete DMEM containing 10% L929 supernatant. Cells were infected as described above with Ye or YeP- for 2 h. Media was aspirated and a 1:1 mix of PBS and Caspase-Glo 8 reagent+buffer (Promega) was added as per the manufacturer's protocol. Plates were allowed to shake at 300 rpm for 40 min before luminescence was read.

Mice. C57BL/6.SJL mice were obtained from Jackson Laboratories. All experiments were performed under Institutional Animal Care and Use Committee (IACUC) approved protocols and in accordance with the guidelines of the IACUC of the University of Pennsylvania. Six- to eight-week-old C57BL/6.SJL mice were lethally irradiated with 1,100 rads and $2-5 \times 10^6$ *Ripk3*^{+/-}*Casp8*^{+/-}, *Ripk3*^{+/-}*Casp8*^{-/-}, *Ripk3*^{-/-}*Casp8*^{-/-} (provided by D.R.G.) and C57BL/6 (Jackson Laboratories) bone marrow (BM) cells were transferred i.v. BM chimeras were allowed to reconstitute for 8 to 10 wk. Mice were starved for 12–16 h and infected orally with $8-10 \times 10^7$ *Yersinia* (32777). Mice were killed and tissues and sera were harvested on days 3, 5, 6, and 7 postinfection, as indicated. Bacterial load was determined by plating dilutions of tissue homogenates on LB+irgasan plates and serum cytokines were measured by sandwich ELISA for IFN- γ (eBioscience).

Flow Cytometry. Spleens and mesenteric lymph nodes were isolated, red blood cells were lysed, and plated in complete-DMEM containing brefeldin A (Sigma) and monensin (BD) in a 37 °C humidified incubator for 5 h. Cells were washed with FACS

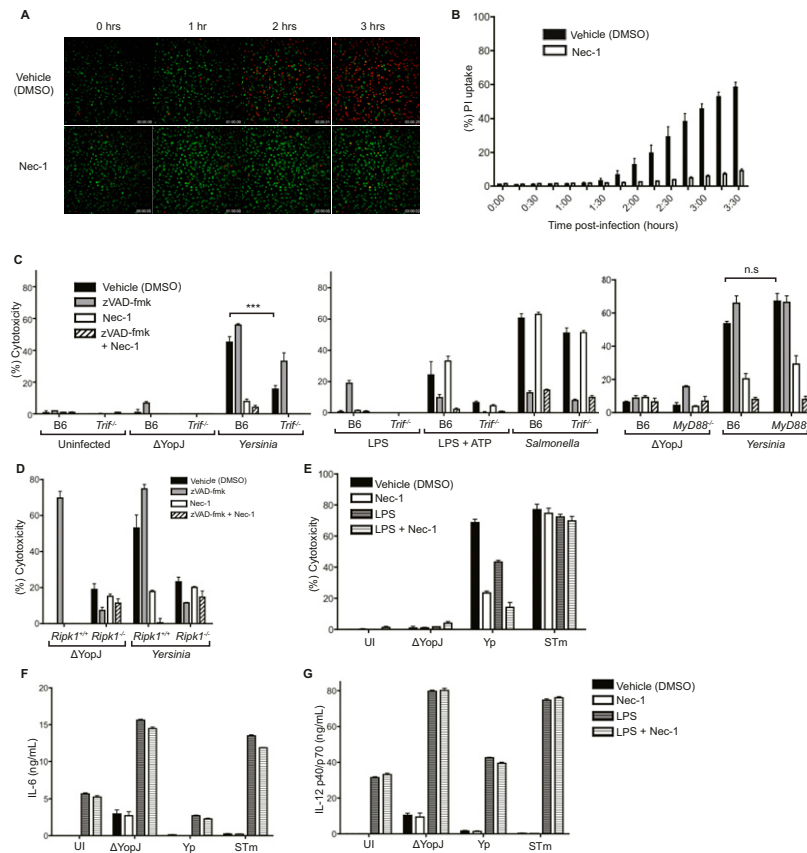
buffer (PBS with 1% BSA and 2 mM EDTA), fixed, and permeabilized (BD) according to manufacturer's instructions and stained for CD19, NK1.1, CD45.1, CD45.2, B220 (BD), CD11b, viability (Invitrogen), Ly6C, CD3, CD11c, TNF, IFN- γ (eBiosciences), and Ly6G (BioLegend). Samples were run on an LSRFortessa and analyzed using FlowJo (TreeStar) software.

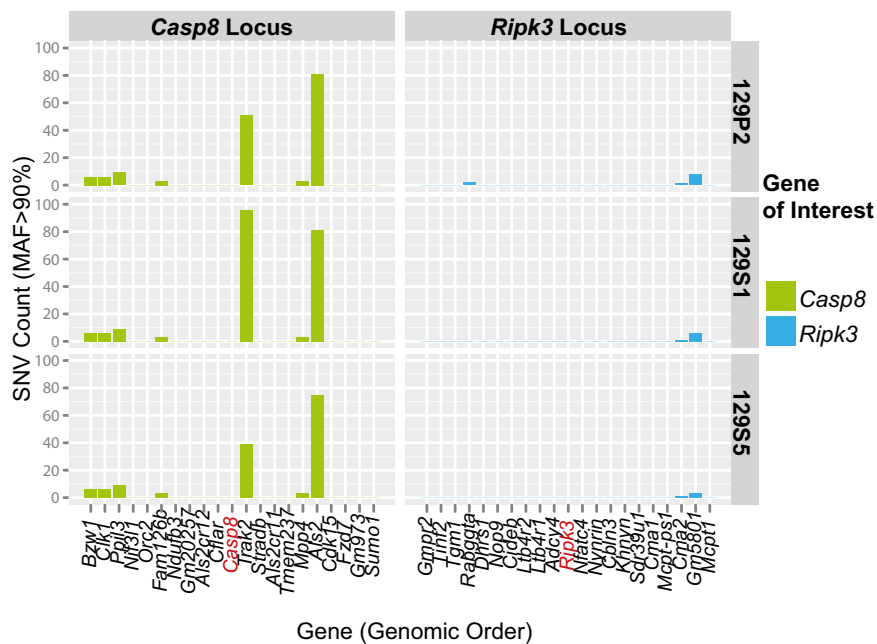
Histopathology. Spleens and livers were fixed and stained for hematoxylin and eosin. Sections were quantified by a blinded pathologist according to the metric in Table S2.

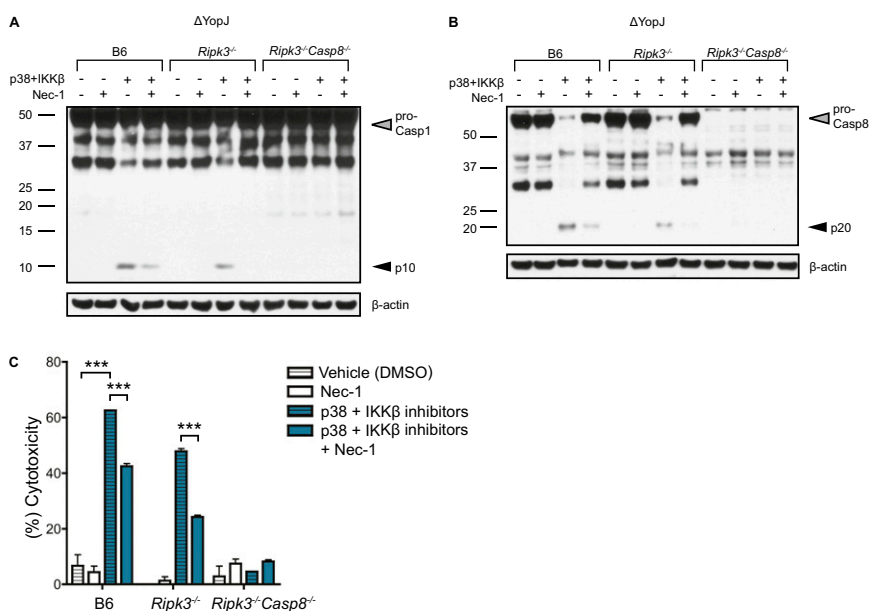
Detection of Germ-Line Single-Nucleotide Variations and Small Insertion/Deletion. We downloaded whole-genome sequencing data from the Mouse Genomes Project of Wellcome Trust Sanger Institute (3). Using a pipeline that was initially developed for detecting somatic mutations using paired tumor/normal sample, we identified the germ-line single-nucleotide variations (SNVs) of the three 129 strains (129P2, 129S1, and 129S5) by running a paired SNV analysis using C57B6 as the reference sample. The initial variant calls were generated using variation detection module of Bambino (4) with the following parameters: -min-flanking-quality 15 -min-alt-allele-count 2 -min-minor-frequency 0 -broad-min-quality 10 -mmf-max-hq-mismatches 15 -mmf-min-quality 15 -mmf-max-any-mismatches 20 -unique-filter-coverage 2 -min-mapq 1. A postprocess pipeline filters SNVs in regions with low-quality regions and remaps (using the program BLAT) and realigns (using the program SIM) the reads harboring variant allele to the mouse mm10 genome to remove additional false calls. The validation rate for human cancer genome analysis is about 95% (5), and that of mouse exome sequencing data are ~90% (6).

Statistics. All statistical analyses were performed using the two-tailed unpaired Student *t* test or Mann–Whitney *U* test, where indicated.

1. Brodsky IE, et al. (2010) A *Yersinia* effector protein promotes virulence by preventing inflammasome recognition of the type III secretion system. *Cell Host Microbe* 7(5): 376–387.
2. Blasi E, et al. (1985) Selective immortalization of murine macrophages from fresh bone marrow by a *raf/myc* recombinant murine retrovirus. *Nature* 318(6047):667–670.
3. Edmonson MN, et al. (2011) Bambino: A variant detector and alignment viewer for next-generation sequencing data in the SAM/BAM format. *Bioinformatics* 27(6): 865–866.
4. Keane TM, et al. (2011) Mouse genomic variation and its effect on phenotypes and gene regulation. *Nature* 477(7364):289–294.
5. Zhang J, et al. (2012) The genetic basis of early T-cell precursor acute lymphoblastic leukaemia. *Nature* 481(7380):157–163.
6. Benavente CA, et al. (2013) Cross-species genomic and epigenomic landscape of retinoblastoma. *Oncotarget* 4(6):844–859.







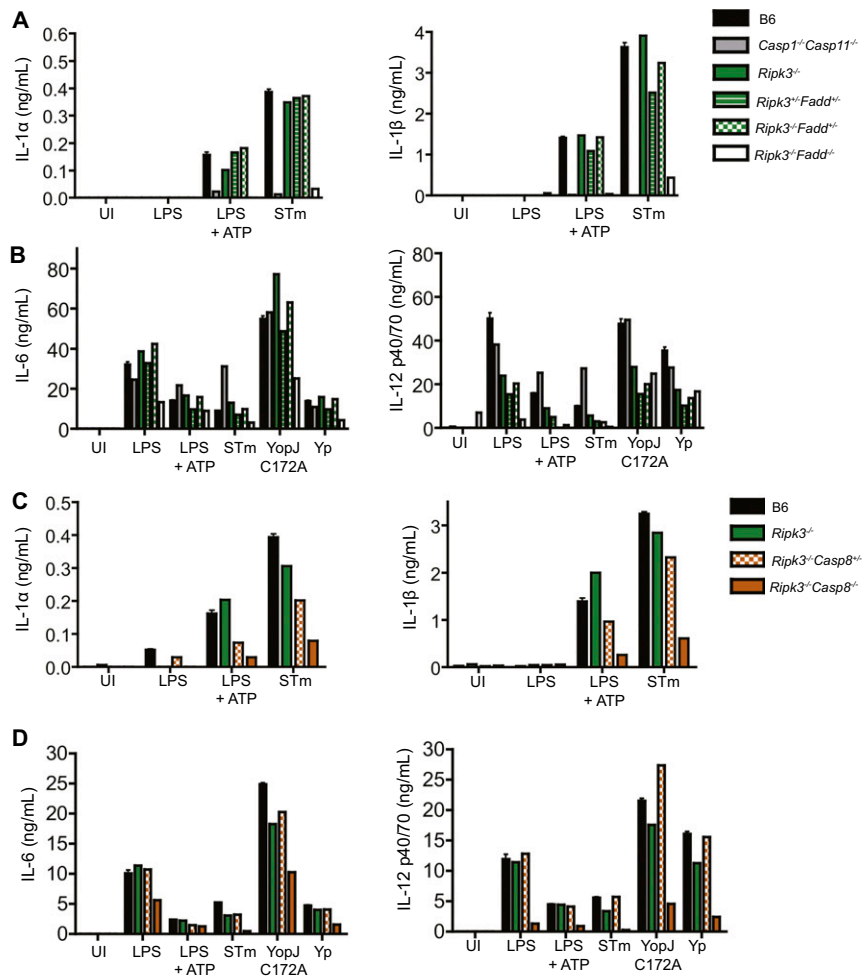
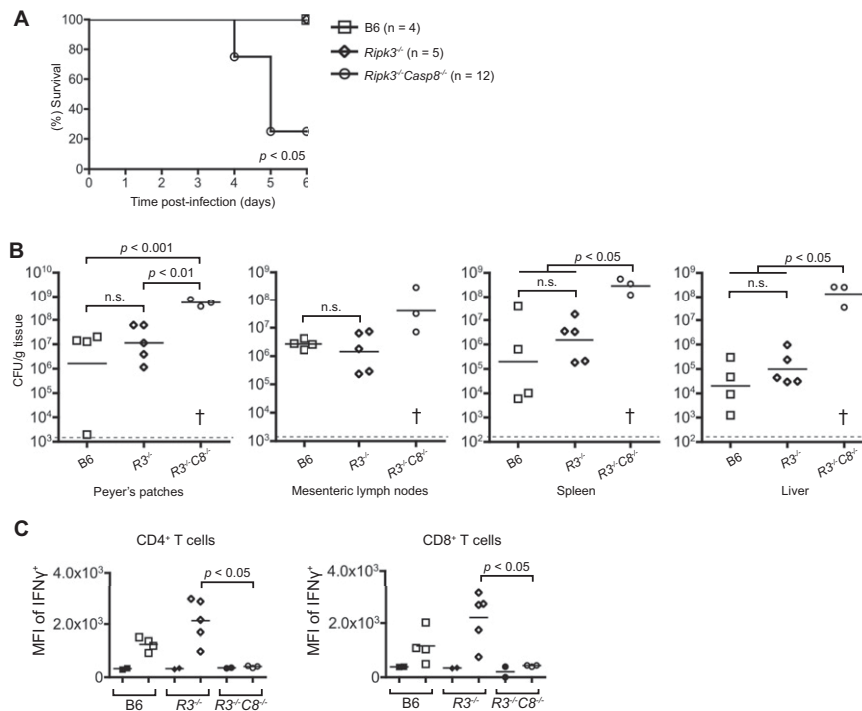


Fig. S7. *Ripk3^{-/-}Casp8^{-/-}* and *Ripk3^{-/-}Fadd^{-/-}* BMDMs have a defect in LPS priming. BMDMs were primed with LPS (50 ng/mL) 3 h before infection with *Yersinia* (YopJ C172A or isogenic 32777, Yp) or *Salmonella*, or treated with ATP (2.5mM) for 4 h. Supernatants were assayed for caspase-1-dependent and -independent cytokine secretion by ELISA. (A and C) IL-1α and IL-1β; (B and D) IL-6 and IL-12p40/70. Error bars indicate mean \pm SEM of triplicates.



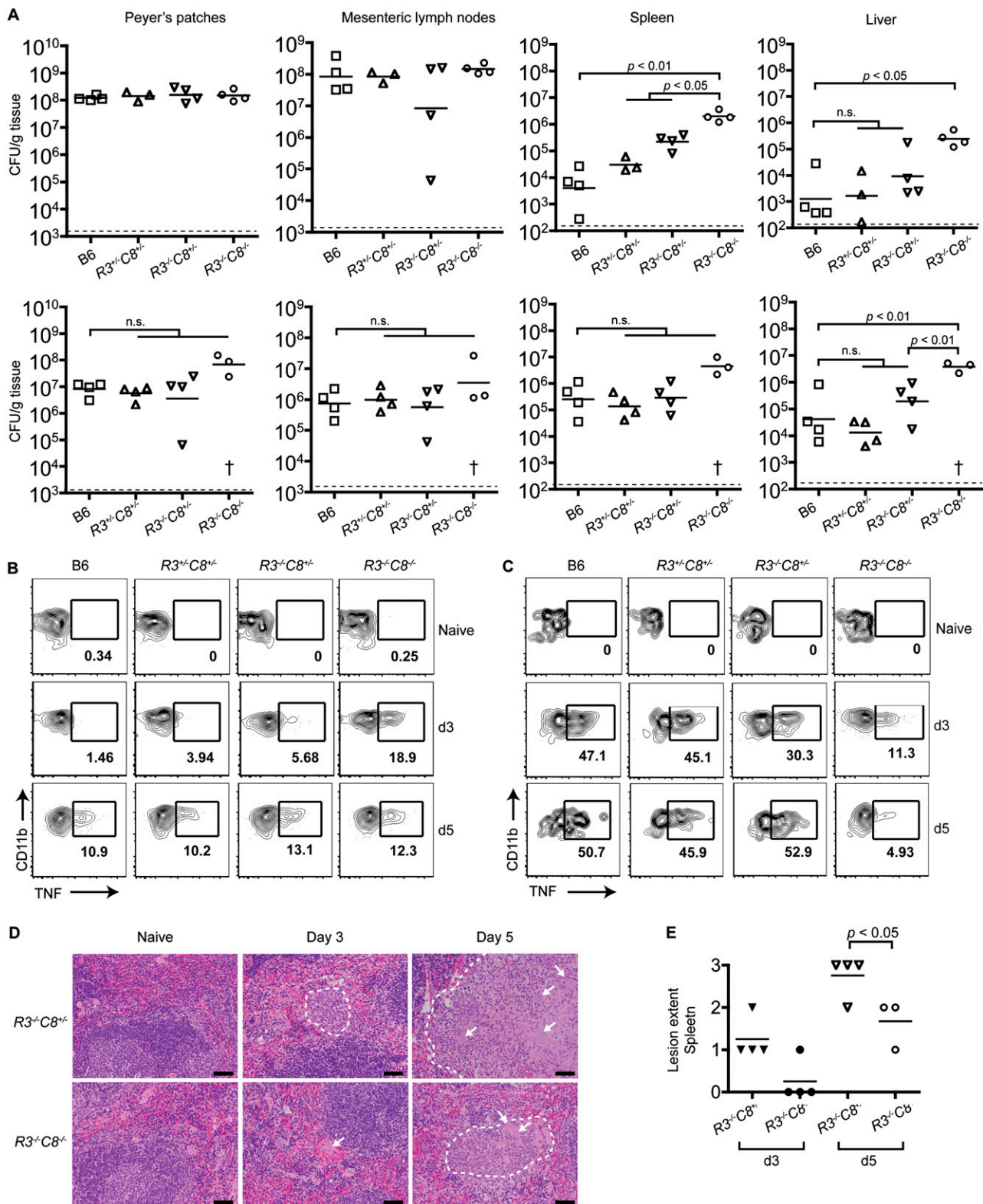


Fig. S9. RIPK3/caspase-8-deficient mice experience faster bacterial dissemination and dysregulated cytokine production even at early time points during *Yersinia* infection. Lethally irradiated B6.SJL mice were reconstituted and infected as in Fig. 4. (A) Bacterial loads per gram of tissue on days 3 (Upper) and 5 (Lower) postinfection. (B and C) Percent TNF⁺ inflammatory monocytes in (B) spleens and (C) mesenteric lymph nodes were analyzed by flow cytometry. (D) Representative images of spleen in naive and *Yersinia*-infected *Ripk3*^{-/-}*Casp8*^{+/+} and *Ripk3*^{-/-}*Casp8*^{-/-} chimeric mice at days 3 and 5, showing lesions of necrosuppurative splenitis (dashed white lines) and extracellular bacterial colonies (arrows) in infected mice. H&E staining. (Scale bars, 50 μ m.) (E) Quantification of lesion severity in spleens. Dagger denotes three dead mice not harvested for cfus. Dotted lines represent limit of detection. Solid lines represent geometric means. Flow cytometry plots were gated on live CD45.2⁺, CD11c⁻, CD11b^{hi}, Ly6G⁻, and Ly6G^{hi}. *R3C8*, *Ripk3Casp8*.

Table S2. Histopathology scoring scheme

Score	No. of lesions	Lesion extent	Bacterial colonies
0	None	None	None
1	0–9	Small	Rare, small
2	10–19	Medium	Infrequent, small to medium
3	20–30	Medium to large, infrequent confluence	Frequent, small to medium
4	>30 or marked confluence	Medium to large, frequent confluence	Frequent, large or coalescing

Rubric that describes the scoring scale for lesion size and number of lesions in spleens and livers of naïve or infected mice.